ZIBELINE INTERNATIONAL PUBLISHING

Earth Sciences Pakistan (ESP)

DOI: http://doi.org/10.26480/esp.02.2020.81.87

ISSN: 2521-2893 (Print)
ISSN: 2521-2907 (Online)
CODEN: ESPADC

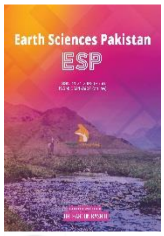

CrossMark

RESEARCH ARTICLE

LANDSLIDE HAZARD IDENTIFICATION (LHI) BASED ON GEOELECTRICAL MAPPING ANALYSIS (GEM): CASE STUDY FROM LUYANG, KOTA KINABALU, SABAH, MALAYSIA

Mohd Fauzi Zikiri[a,b], Rodeano Roslee[b,c]*, Ahmad Nazrul Madri[a,b]

[a] Department of Public of Work (Sabah State), Slope Branch, Sembulan Road, 88538 Kota Kinabalu, Sabah, Malaysia.
[b] Universiti Malaysia Sabah, Faculty of Science and Natural Resources, UMS Road, 88400 Kota Kinabalu, Sabah, Malaysia.
[c] Universiti Malaysia Sabah, Natural Disaster Research Centre (NDRC), UMS Road, 88400 Kota Kinabalu, Sabah, Malaysia.
****Correspondence Author Email: rodeano@ums.edu.my***

ARTICLE DETAILS

Article History:

Received 29 September 2020
Accepted 30 October 2020
Available online 18 November 2020

ABSTRACT

Landslides are amongst the most damaging natural hazards in Malaysia. The study of landslides has drawn nationwide attention mainly due to increasing awareness of the socio-economic impact of landslides, as well as the increasing pressure of urbanization. Landslide Hazard Identification (LHI) is part of the process used to evaluate if any particular situation, item, thing, etc. may have the potential to cause harm. The description of LHI should include the location, volume (or area), classification and velocity of the potential landslides and any resultant detached material, and the probability of their occurrence within a given period of time. In this paper, we present the results of the measurement for the subsurface resistivity within by using the pole-dipole electrode array and present the 2D view of each resistivity profile. The result presented successfully detect the dominant layer consists of interbedded sandstone and shale of the Crocker Formation with highly weathered. This both layers have high porosity and potential to contain high water content which can trigger landslide to occur. Besides that, there are several boulders zone (weathered to fresh rock) that can be found at the top of the subsurface profile at about 1.5m to 15m in depth. The bedrock layer was estimated to be found at 4m to 32.5m in depth from the original ground and one possible fault line that had been identified. This fault line believed plays a role in the occurrence of landslide in which rock materials have lower strength compared to surrounding rocks. High density of fault means lower stability. Therefore the faut line have been regarded as a critical factor in triggering landslide in the study area. The results of these study findings are expected to be used as uniform guidelines and principles are very useful and have integrity in providing coordination of standards or policies for each planning activities for new development in the future. As a result of the lack of concern for the developer of the concept of Sustainable Development Goals (SDG) or balancing and control of environmental health, the results of this study can also be used as a yardstick to party developers who intend to develop a high ground and hillside in deciding whether to continuing development planning or not.

KEYWORDS

Landslide Hazard Identification (LHI), Geoelectrical Mapping Analysis, Kota Kinabalu.

1. INTRODUCTION

Landslides are influenced by many factors that range from the intensity, duration and extent of a triggering factor (e.g. earthquake and rainfall) to the local physical conditions such as landform, morphological, geological materials and structures, hydrological and land uses (Varnes, 1978; Crozier, 1986; Popescu, 2002; Guzzetti, 2002; Crozier and Glade, 2005). Thus, a landslide is rarely attributed to a single causal factor (Varnes, 1978). Popescu explained that an analysis of landslide causes should include the 'causal' factor and also the 'process' factor (Popescu, 2002). For example, ground with sensitive fabric, fracturing and highly weathered material are influential criteria (process factors) for the instability of ground and not the main causes of a landslide. However, when environmental factors such as high pore-water pressure (causal factors) are added, failure may occur. These environmental factors are the main cause (in terms of preparation and triggering) of landsliding.

Reconnaissance methods in landslides study, which mainly include remote-sensing and aerial techniques, geological and geomorphological mapping, geophysical and geotechnical techniques, have to be adapted to the characteristics of the landslide. According to a study, geophysical and geotechnical appraisal of landslide's stability has to consider three following issues: (1) the definition of the 3D geometry of the landslide with particular reference to failure surfaces, (2) the definition of the hydrogeological regime, (3) the detection and characterisation of the movement (McCann and Foster, 1990). Except in very peculiar cases, a landslide generally results in a modification of the morphology and of the internal structure of the affected ground mass, both in terms of hydrogeological and mechanical properties.

Quick Response Code	Access this article online	
	Website: www.earthsciencespakistan.com	**DOI:** 10.26480/esp.02.2020.81.84

Cite The Article: Mohd Fauzi Zikiri, Rodeano Roslee, Ahmad Nazrul Madri (2020).Landslide Hazard Identification (Lhi) Based On Geoelectrical Mapping Analysis (Gem): Case Study From Luyang, Kota Kinabalu, Sabah, Malaysia. *Earth Sciences Pakistan, 4(2): 81-84.*

The main target of Geoelectrical Mapping Analysis (GEM) methods prospecting for landslide investigation is particularly depends on a type of the rocks, water contents and its mineralization. Electric resistivity decreases with increasing contents of water in the rock and with increasing mineralization of water (Telford et al., 1990). On the other hand, resistivity increases with an increasing grain size of the rock. This means that resistivity measurements can be used to separate individual structural elements of the rock massive and to observe changes in time. As varying with time there may be a factor of moisture content. The water gradually infiltrates into a medium and reduces its resistivity. Examples of resistivity measurements in landslide, these measurements based on four-electrode measuring systems. The interpretation was made for complicated geoelectric conditions, for the zone between the ground level and bedrock (or reaching a depth of around 30 m below the ground level). Deeper areas below the ground level are screened by near-surface effects and the imaging of bedrock changes is therefore somewhat simplified.

2. Background of The Study Area

Rapid economic development in Luyang area, Kota Kinabalu, Sabah, Malaysia resulted in further pressure to utilize the slope land for various purposes such as recreation, infrastructure and human settlements (Figure 1). Topographic setting of the study area is controlled mainly by its hilly areas and very limited flat planes. Under this situation it could not avoid the opening of slope lands for development projects. It is important that the inherent physical and environmental constraints in an area should be recognized. Only then proper mitigation could be planned and applied. This is to ensure the sustainable long-term development of slope lands and to avoid over exploitation and mismanagement.

Several cases of catastrophic events landslide occurred in the study (Figure 2). For example, on 10th June 2010 in the nearest place had been a two landslide incidents at KM 1.95 and KM 2.50 (Figure 2a), destroyed one wooden houses and other property losses estimated at close to thousands ringgit. In addition, the embankment failure on 13th October 2014 at KM 1.20 and KM 1.35 also gives a impact on the local population, which caused disruption of communication system (Figure 2b). The immediately instructions forprecautionary measuresbecause of slope failure feature also occurred in Jalan Penempatan area, such as at KM 1.10 and several luxurious residential areas, for example at KM 1.88 which had to be need intensively monitored because is found to be unstable and recommended could lead to the occurrence of disaster landslide (Figure 2c). This does not include a number of existing landslide prone area cases along theJalan Penempatanarea that have yet taken any action or well managed by the local authorities which are landsliding process still active and continue to occur.

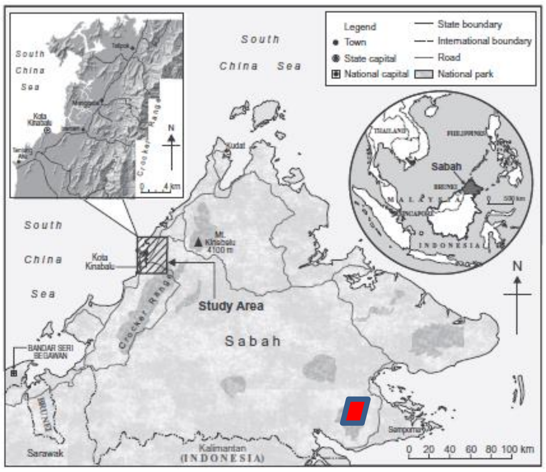

Figure 1: Location of the study area

Figure 2: Landslide occurrences in the study area

The geology of the study area is made up of sedimentary rock of the arenaceous Crocker Formation (Late Eocene age) and Quaternary Alluvium Deposits (Figure 3). Table 1 shows the composite stratigraphic column of rock units with their water bearing and engineering properties. The layered nature of the sandstone and shale of the Crocker Formation are generally oriented between N325E to N010E and show steep dips (40-

85 degrees) eastward. Large scale folds (> 100 meter wavelength), faults (several meters wide) and more than four (4) set joints orientation are common in the study area.

The sandstone-shale contact is easily accessible by water and such contact seepage may weaken the shale surface and cause slides and falls within the formation. Interbedded sandstone and shale may also present problems of settlement and rebound. The magnitude, however, depends on the character and extent of shearing in the shale. The strength of the sandstone will also depend on the amount and type of cement-matrix material occupying the voids. The sandstones are compacted and in grain to grain contact with each other. Instead of chemical cement (vein) or matrix, the pores are filled by finer-grained sands to silt-sized materials or squeezed rock fragments. The absence of chemical cement reduces the strength of the sandstone especially when it is weathered or structurally disturbed (Rodeano et al., 2006, 2011, 2017; Rodeano 2019).

The shale units have an adequate strength under dry conditions but lose this strength when wet (Rodeano et al., 2006, 2011, 2017; Rodeano 2019). During the rainy season, the shale becomes highly saturated with water which increases the water pressure and reduces resistances to sliding and falling especially within the sandstones-shale contact. This condition, in addition to varying amounts of bitumen and levels of degradation, makes shale unpredictable and unsuitable for road construction sites. Its unstable nature can be remedied by proper management of soaking and draining of water from the rock or along the sandstone-shale contact.

The alluvium is mainly represent unconsolidated alluvial sediment on river terraces and weathered product materials composed of unsorted to well-sorted, sand, silt and clay of varying proportions which were derived from the bed rocks. They occur in irregular lenses varying in the form and thickness. The alluvium may also consist of very thin layer of organic matter and characterized as soft, compressible and may be prone to settlement (Rodeano et al., 2006, 2011, 2017; Rodeano 2019).

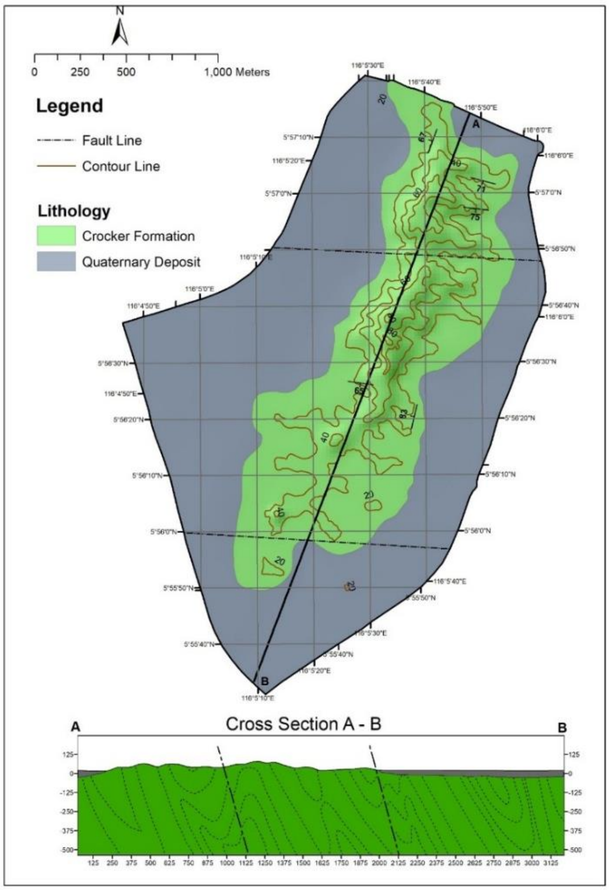

Figure 3: The geology map of the study area

Table 1: Local Stratigraphic Column and their lithological characteristics (After: Rodeano and Felix, 2018a; 2018b & 2018c).

3. Material and Methods

The main component for Geoelectrical Mapping Analysis (GEM) is transmitter, receiver and DC power supply. This survey will utilize the multi-electrode survey with five meters spacing (usually 41 to 61). Pole-dipole electrode array (Figure 4) used with ABEM Terrameter SAS4000 in this ERI for deeper penetration. Electrodes laid out in a straight line with a constant 5 meters spacing (Figure 5). A computer-controlled system use to automatically select the active electrodes for each measure (Griffith and Barker, 1993). The data collected in the survey will be processed using software RES2DINV.

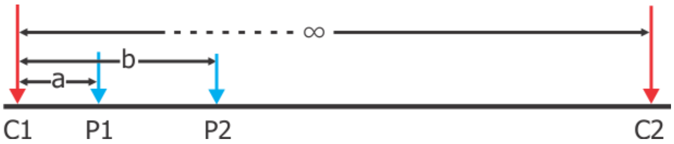

Figure 4: Pole-dipole Electrode Array

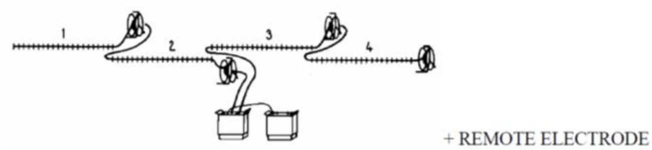

Figure 5: Terrameter SAS4000 Arrangement with four Lund Cable

The GEM measurements are normally made by injecting direct current (DC) into the ground through two current electrodes (C1 and C2) and measuring the resulting voltage difference at two potential electrodes (P1 and P2). From the current (I) and voltage (V) values, an apparent resistivity (ρa) value is calculated.

$$\rho a = k\frac{V}{I}$$

Where k is the geometric factor which depends on the arrangement of the four electrodes. Resistivity meters normally give a resistance value, R = V/I, so in practice the apparent resistivity value is calculated by ρa = k R = 2πa ΔV/I. The calculated resistivity value is not the true resistivity of the subsurface, but an "apparent" value which is the resistivity of a homogeneous ground which will give the same resistance value for the same electrode arrangement. The relationship between the "apparent" resistivity and the "true" resistivity is complex.

To determine the true subsurface resistivity, an inversion of the measured apparent resistivity values using a computer program has been carried out. One of the new developments in recent years is the use of 2D geoelectrical resistivity imaging/tomography surveys to map areas with moderately complex geology (Griffiths and Barker, 1993). Such surveys are usually carried out using a large number of electrodes connected to a multi-core cable. A modern resistivity meter together with an electrode selector system is used to automatically select the relevant four electrodes for each measurement.

4. Results and Discussion

In this study, five (5) survey lines were studied as illustrated in Figure 6. The orientation for line UBH01 is NW to SE, line UBH02 is SSW to NNE, line UBH03 is W to E, line UBH04 is SW to NE and line UBH05 is N to S. One of the most vital factor to prepare the survey line is the accessibility of the sites especially in urban area. The survey were using protocol pole dipole 4 short (pd4s) for it's configuration set up because of the limited access of the site but still gain enough data to produce the pseudosection.

Figure 6: Distribution line resistivity survey.

Table 1: local stratigraphic column and their lithological characteristics (after: rodeano and felix, 2018a; 2018b & 2018c).

Rock Formation	**Lithologic Units**	**Average Thickness (cm)**	**General Character**	**Water-Bearing Properties**	**Engineering Properties**	*Petrology*	**Sedimentary Structures**	**Fossil**	**Depositional Mechanism**	**Depositional Environment**
Alluvium and Colluvium	Alluvial terraces and flood plains	-	Unconsolidated gravel, sand and silt with minor amounts of clay deposited along the rivers or streams and their tributaries. Includes natural levee and flood plain deposit.	Gravelly and sandy, portions are highly permeable and yield large quantities of water. Important to groundwater development.	Generally poorly consolidated. Hence not suitable for heavy structures and subsidence under heavy load.	Angular to sub rounded sandstone blocks in a silty matrix	-	-	Alluvial terraces and flood plains	-
Crocker Formation	Massive Sandstone (Facies B)	100 – 1,000	Light grey to cream colour, medium to course -grained and some time pebbly. It is highly folded, faulted, jointed, fractured occasionally cavernous, surfically oxidized and exhibits spheriodal weathering.	Importance to groundwater.	Good site for heavy structures with careful investigation. Stable from mass movement and provide some modification like closing of continuous structure.	Quarzarenite and Sublitharenite (Immature)	Inorganic Structures *Pre – depositional* 1. Climbing Ripple 2. Ripple Marks 3. Tool Marks 4. Scour Marks *Syn – depositional* 1. Bedding 2. Lamination 3. Graded bedding 4. Cross bedding 5. Convolute lamination *Post – depositional* 1. Slump structures 2. Soft sediment fault 3. Lutite clasts 4. Load structures 5. Ball and pillow structures 6. Water escapes structures **Organic Structures** Plant remains **Trace fossil** *Pre – depositional traces* **1.** *Paleodictyon minimum Cosmorhaphe sinuosa* *Post – depositional traces* 1. Post – depositional burrow type 1 2. Post – depositional burrow type 2 3. Post – depositional burrow type 3 4. Post – depositional burrow type 4 5. Post – depositional burrow type 5	1. Bathysiphon spp 2. Glomospira sp 3. Cyclammina cancellata (Brady) 4. Haplophragmoideswalteri (Grzybowski) 5. Trochamminoides sp.	Grain flow deposits	Upper fan to Middle fan
	Thick bedded Sandstone (Facies C)	10 – 50 (Sandstone) 1 – 15 (Shale)	It is a sequence of interlayering of permeable sandstone with impermeable shale. The permeability of this unit is quite variable.	Groundwater in this unit tends to be under semi-confined to confined system. Little importance to groundwater provides some water but not enough for groundwater development.	Dangerous site for heavy structures and high potential for mass movement.	Moderately well sorted to moderately sorted (Mature and Immature)			High density, high velocity turbidity currents (Proximal turbidites)	Outer fan localized in channels and in the prograding depositional lobes.
	Thin bedded Sandstone (Facies D/E)	3 – 5 (Sandstone) 5 – 10 (Shale)							Waning or low velocity turbidity currents (Distal turbidites)	Middle to outer fan and particularly basin plain
	Slumped (Facies F)	-	This unit is composed of two types of shale red and grey. It is a sequence of alteration of shale with siltstone of very fine.	It has no significant to groundwater development due to its impermeable characteristic.	Very dangerous site for heavy structures and the main causes of mass movement.	-			Turbidite and debris flow sedimentation	Shelf to lower slope and partly in the channels of inner fan, middle fan and basin plain
	Red / Grey Shale (Facies G)	1 – 2 (Siltstone) 10 – 50 (Mudstone)				-			Debris flow	Plain basin, middle fan and slope region

Cite The Article: Mohd Fauzi Zikiri, Rodeano Roslee, Ahmad Nazrul Madri (2020).Landslide Hazard Identification (Lhi) Based On Geoelectrical Mapping Analysis (Gem): Case Study From Luyang, Kota Kinabalu, Sabah, Malaysia. *Earth Sciences Pakistan, 4(2): 81-84.*

The results of the survey shown in attachment 1 to 5 in two dimensional (2D) sections known as pseudo-section for the Resistivity 2D Imaging. The range of resistivity value shown in color scheme bar. The lithology description of the resistivity (ohm-m) color scheme bar are referred to the borehole log provided. Based on the resistivity value, we can differentiate the zoning layer within the subsurface into three (3) types:

1. Resistivity value less than 100 Ωm as highly water content zone. The materials of this layer are sandstone, silt, and clay.
2. Resistivity value of 100 Ωm to 1,000 Ωm as weathered rocks with less water content. The materials of this layer are weathered sandstone, silt, and clay.
3. Resistivity value of greater than 1,000 Ωm is classified as fresh to moderate weathered Sandstone, silt, and clay with no water content. It can be interpreted as bedrock of Crocker Formation.

4.2 UBH01@G04

The resistivity line was oriented northwest - southeast (Figure 6). The cable was spread in such that point A was facing northwest while point B was facing southeast. The length of line resistivity is 120m. Figure 7a shows the view of the study area where the survey line resistivity 1 was conducted which near to BH01. The pseudo-section shows the result of resistivity survey for line 1. Based on the zoning, the subsurface consists of material of highly water content, the weathered sandstone and fresh mudstone or shale. The highly water content is represented by the low resistivity value. At the left part of the pseudo-section, the highly water content is situated within 15m from the surface. Beyond the center, the highly water content zone can reach up until 40m thick. The bottom of the pseudo-section is dominated by weathered sandstone on the left side of the profile. Fresh rock or hard layer, represented by high resistivity value can be found mainly on the right side of the pseudo section. The thickness of the hard layer is about 17m (Figure 7b).

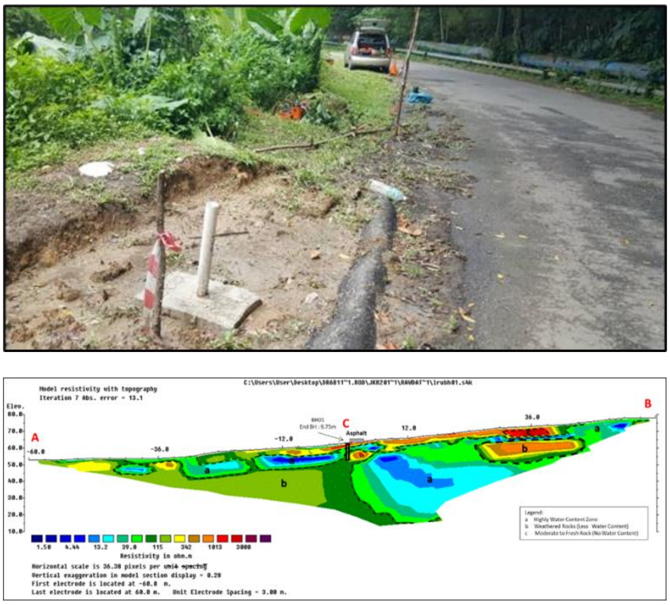

Figure 7: General view of the survey area line resistivity and resistivity 2D Imaging Pseudosection result for Survey Line UBH01@ G04.

4.3 UBH02@G03

The resistivity line was oriented south-southwest –north-northeast (Figure 6). The cable was spread in such that point A was facing south-southwest while point B was facing north-northeast. The length of line resistivity is 120m. Figure 8a shows the view of the study area where the survey line resistivity 2 was conducted which near to BH02. The result shows the subsurface profile for resistivity survey line 2. Based on the pseudo section, the fresh bedrock layer is dominant. The layer of highly water content is also present in the profile. The top left layer in the pseudo section consists of a boulder of rock underlain by a layer of highly water content. The thickness of the boulder is only about 3m to 5m while the thickness of highly water content zone is about 12m. The bedrock layer is observed at bottom of the pseudo section and the thickness of this zone at the center line is 47m. At 12m from the center towards point B, a zone of highly water content with 9m width and 11m thick is identified. Adjacent to the zone is the boulder zone. There is one possible fault that had been identified which is located at distance 12m (Figure 8b).

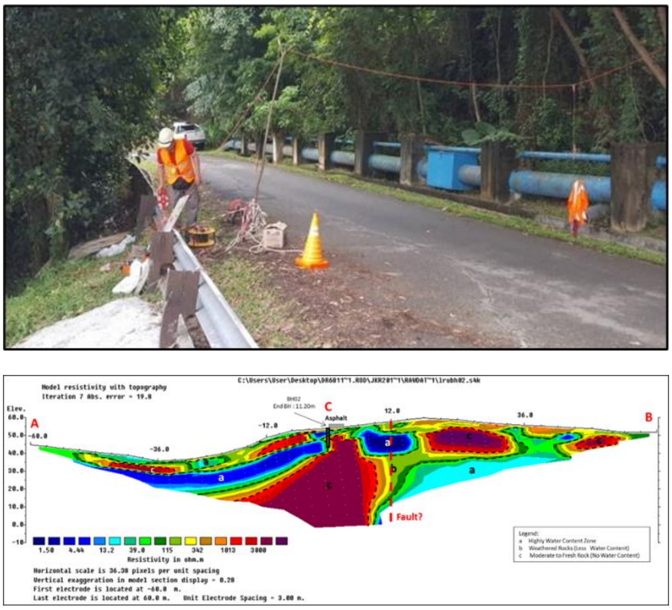

Figure 8: General view of the survey area line resistivity and resistivity 2D Imaging Pseudosection result for Survey Line UBH02@ G03.

4.4 UBH03@G02

The resistivity line was oriented west – east (Figure 6). The cable was spread in such that point A was facing west while point B was facing east. The survey line resistivity 3 (200m) was conducted which near to BH03. The pseudo section shown in this figure represents the subsurface profile for resistivity survey line 3. A few zones in this profile show the presence of boulder occurrences. These boulders mainly are found on the top layer of the subsurface within the range of 11m below the ground level. The boulders show varieties of thickness, from 2.5m to 9m. Apart from that, these boulders zone also shows different resistivity value, and this may be influenced by the degree of weathering or fracturing of the rock. The result shows that on this survey line, most of the subsurface condition is wet. The highly water content zone is more concentrated at the middle of the pseudo section. In term of depth, the high water content can be encountered at minimum depth of 7m. At the center of the survey line, the upper layer of the pseudo section represented by low resistivity value, which also suggest the occurrences of highly water content. The highly water content zone is underlain by the layer of bedrock. This bedrock is found at approximately 30m depth (Figure 9a & 9b).

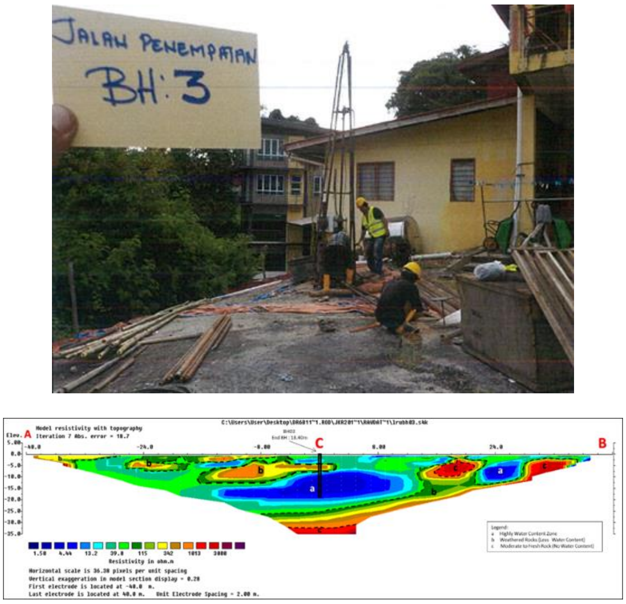

Figure 9: General view of the survey area line resistivity and resistivity 2D Imaging Pseudosection result for Survey Line UBH03@ G02

4.5 UBH04@G01

The resistivity line was oriented southwest –northeast (Figure 6). The cable was spread in such that point A was facing southwest while point B was facing northeast. The length of line resistivity is 80m. Photo 7 shows the view of the study area where the survey line resistivity 4 was conducted which near to BH04. The subsurface profile for line 4 is interpreted to consist of material with low resistivity value. The maximum value of resistivity determined in this survey line is less than 400Ωm. Two zone are identified within this subsurface profile according to their resistivity value. The zone of highly water content zone is enormous and cover almost the entire subsurface profile. This zone reach the bottom of the pseudo section at 110.0m distance from point A towards point B. Towards point A, the highly water content layer is underlain by the zone of weathered rock which is less fractured and less water content. This layer is measured to be found at 30m depth (Figure 10a and 10b).

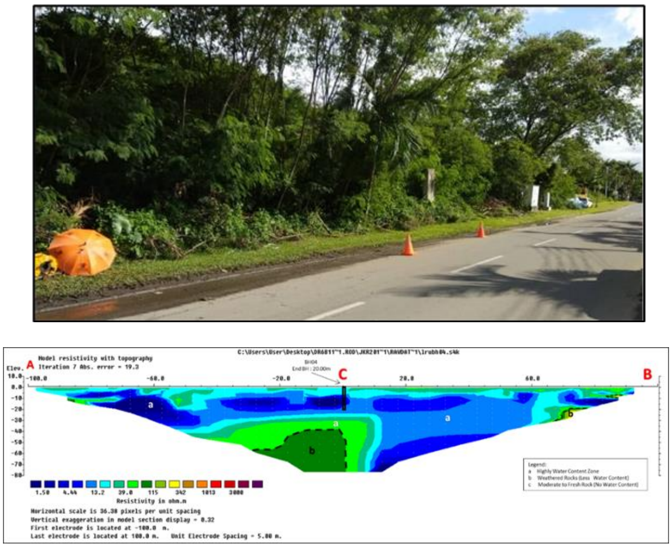

Figure 10: General view of the survey area line resistivity and resistivity 2D Imaging Pseudosection result for Survey Line UBH04@ G01

4.6 UBH05@G05

The resistivity line was oriented north – south (Figure 6). The cable was spread in such that point A was facing north while point B was facing south. The length of line resistivity is 100m. Figure 11a shows the view of the study area where the survey line RES 5 was conducted which near to BH05. The pseudo section of resistivity survey line 5 shows the occurrence of highly water content, weathered or fractured rock and fresh rock. The layer of fresh rock is found at the top right layer in the pseudo section. This layer has estimated thickness about 10m in average. The zone of possible boulders can be traced at 35.0m distance from point A. This zone has a thickness of 11m, width of 5m and located 4m below the surface. At 40.0m to 52.0m distance from point A, the zone of highly water content is pinpointed underneath the fresh rock layer. The measured thickness of this zone is 8m. A small scale zone of high water content is spotted at 38.0m distance from point A and probably have connection with the former. In general, the highly water content zone can be encountered at a shallower depth at point A area and at a deeper depth at point B area, within the range of 3m to 14m (Figure 11b).

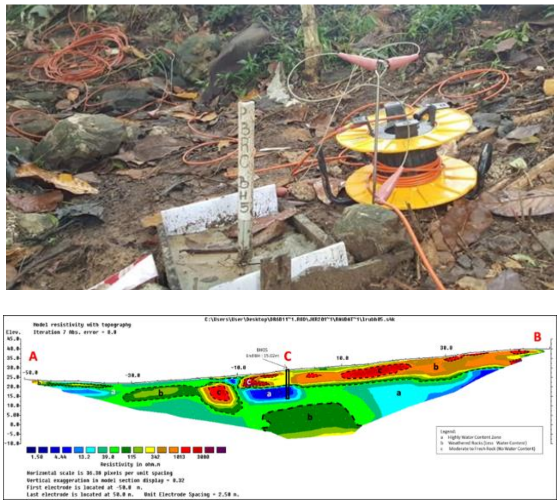

Figure 11: General view of the survey area line resistivity and resistivity 2D Imaging Pseudosection result for Survey Line UBH05@ G05.

5. Conclusion

In light of available information, the following conclusions may be drawn from the present study:

1. The geoelectrical resistivity of subsurface layers is influenced by: a) Lithology of the layers, i.e. the material composition, either geoelectrically conductive or non-conductive; b) Porosity of the layers, together with the nature of the content of the pore spaces, whether water or air, the degree of water saturation and the dissolved material in the water; and c) Degree of consolidation, weathering and degree of fracturing of the rock mass.
2. Three general type of material can be classified based on resistivity values. Table 2 show description layer of subsurface profile.

Table 2: Description layer of subsurface profile

ITEM	DESCRIPTION LAYER	RESISTIVITY VALUE (Ωm)	TYPE OF SOIL
a	Highly Water Content Zone	0 - 100	SAND / SILT
b	Weathered Rock (Less Water Content)	100 - 1000	CLAY / SILT
c	Moderate to Fresh Rock (No Water Content)	> 1000	Sandstone / Shale

3. Based on the pseudosection, the dominant layer consists of interbedded sandstone and shale with highly weathered. This both layer have high porosity and potential to contain high water content. This layer can be found from the top of subsurface until depth more than 35m.

4. There are several boulders zone (weathered to fresh rock) that can be found at the top of the subsurface profile as shown in pseudo section UBH01@G04, UBH02@G03, UBH03@G02and UBH05@G05. The thickness of this boulder zone is about 1.5m to 15m.

5. Bedrock layer was estimated to be found at 4m to 32.5m depth from the original ground as show in subsurface profile line resistivity UBH02@G03 and UBH03@G02. There is one possible fault that had been identified at survey line UBH02@G03. This fault line believed plays a role in the occurrence of landslide in which rock materials have lower strength compared to surrounding rocks. High density of fault means lower stability. Therefore the faut line have been regarded as a critical factor in triggering landslide in the study area.

6. Groundwater levels from below the existing ground level in all the boreholes were also measured at the time of site investigation works. It should be noted that, the measured groundwater levels when boring works stopped could be due to retention of water used in the process of boring works. However, the measurements conducted in the overnight mornings or after the completion of boring works could be the actual phreatic water levels. Also the groundwater levels in boreholes may vary owing to seasonal or other effects. Based on monitoring, groundwater level at BH-1 is ranges from full to 3.59 m, BH-2 is ranges from 2.73 to 6.31 m, BH-3 is ranges from 2.70 to 4.70 m, BH-4 is ranges from 0.40 to 0.60 m and BH-5 is ranges from 3.90 to 4.20 m.

7. The results of these study findings are expected to be used as uniform guidelines and principles are very useful and have integrity in providing coordination of standards or policies for each planning activities for new development in the future. As a result of the lack of concern for the developer of the concept of Sustainable Development Goals (SDG) or balancing and control of environmental health, the results of this study can also be used as a yardstick to party developers who intend to develop a high ground and hillside in deciding whether to continuing development planning or not.

Acknowledgements

Deep gratitude to Universiti Malaysia Sabah (UMS) for providing easy access to laboratories and research equipment. Highest appreciations also to Public of Work (Sabah State) for the research grant award (*Pemetaan Bahaya dan Risiko cerun di Jalan Penempatan, Kota Kinabalu bagi projek kajian dan lukisan (cerun) di bawah vot peruntukan D33 dalam RMK11*) to finance all the costs of this research.

References

Crozier, M.J., 1986. Landslides Causes, Consequences & Environment. Croom Helm: London.

Crozier, M.J., Glade, T., 2005. Landslide hazard and risk: issues, concepts and approach. In. Glade, T., Anderson, M. & Crozier, M.J (Eds.), Landslide Hazard and Risk. John Wiley & Sons: Chichester. Pp. 1-40.

Guzzetti, F., 2002. Landslide Cartography, Hazard Assessment and Risk Evaluation: Overview, Limits and Prospective. Proceedings of 3rd MITCH Workshop Floods, droughts and landslides who plans, who pays. Potsdam, Germany.

MC Cann, D.M., Forster, A., 1990. Reconnaissance geophysical methods in landslide investigations. Eng. Geol., 29, Pp. 59–78.

Popescu, 2002. Landslide causal factors and landslide remedial options, keynote lecture. Proc. of the Third International Conference on Landslides, Slope Stability and Safety of Infra-Structures, Singapore. Pp. 61-81.

Rodeano, R., 2019. Engineering Geological Investigation on Karambunai-Lok Bunuq Landslides, Kota Kinabalu, Sabah. Malaysian Journal of Geosciences, 3 (2), Pp. 01-06.

Rodeano, R., Felix, T., 2018a. Engineering Geological Assessment (EGA) on Slopes Along The Penampang to Tambunan Road, Sabah, Malaysia. Malaysian Journal of Geosciences, 2 (1), Pp. 06-14.

Rodeano, R., Felix, T., 2018b. Engineering geological study on the slope failure along the Kimanis to Keningau highway, Sabah, Malaysia. Geo. Behav., 2 (2), Pp. 01-09.

Rodeano, R., Felix, T., 2018c. Engineering Geological Mapping on Slope Design in the Mountainous Area of Sabah Western, Malaysia. Pakistan Journal of Geology, 2 (2), Pp. 01-10.

Rodeano, R., Sanudin, T., Omang, S.A.K.S., 2006. Engineering Geology of the Kota Kinabalu Area, Sabah, Malaysia. ISSN 0126-6187. Bull. Geol.Soc. Malaysia., 52, Pp. 17-25.

Rodeano, R., Tajul, A.J., Mustapa, A.T., 2011. Aplikasi GIS dalam Penaksiran Risiko Gelinciran Tanah (LRA): Kajian Kes bagi kawasan sekitar Bandaraya Kota Kinabalu, Sabah, Malaysia. Bull. Geol. Soc. Malaysia, 57, Pp. 69-83.

Rodeano, R., Norbert S., Felix, T., Mohd. Norazman, N., Mohd, R.T., 2017. Landslide Susceptibility Analysis (LSA) using Deterministic Model (Infinite Slope) (DESSISM) in the Kota Kinabalu Area, Sabah, Malaysia. Geo. Behav., 1 (1), Pp. 06-09.

Telford, W.M., Geldart, L.P., Sheriff, R.E., 1990. Applied Geophysics. Cambridge F U.P., Cambridge.

Varnes, D.J., 1978. Slope movement types and processes, landslides analysis and control. Special Report 176. Transportation Research Board, Washington, DC, Pp. 11–80.